

Assessing the Performance of a Three Dimensional Hybrid Central-WENO Finite Difference Scheme with Computation of a Sonic Injector in Supersonic Cross Flow

Wai-Sun Don^{1,*}, Antonio de Gregorio², Jean-Piero Suarez² and Gustaaf B. Jacobs²

¹ *Department of Mathematics, Hong Kong Baptist University, Kowloon Tong, Hong Kong*

² *Department of Aerospace Engineering & Engineering Mechanics, San Diego State University, 5500 Campanile Drive San Diego, CA 92182, USA*

Received 12 March 2012; Accepted (in revised version) 28 August 2012

Available online 9 November 2012

Abstract. A hybridization of a high order WENO-Z finite difference scheme and a high order central finite difference method for computation of the two-dimensional Euler equations first presented in [B. Costa and W. S. Don, *J. Comput. Appl. Math.*, 204(2) (2007)] is extended to three-dimensions and for parallel computation. The Hybrid scheme switches dynamically from a WENO-Z scheme to a central scheme at any grid location and time instance if the flow is sufficiently smooth and vice versa if the flow is exhibiting sharp shock-type phenomena. The smoothness of the flow is determined by a high order multi-resolution analysis. The method is tested on a benchmark sonic flow injection in supersonic cross flow. Increase of the order of the method reduces the numerical dissipation of the underlying schemes, which is shown to improve the resolution of small dynamic vortical scales. Shocks are captured sharply in an essentially non-oscillatory manner via the high order shock-capturing WENO-Z scheme. Computations of the injector flow with a WENO-Z scheme only and with the Hybrid scheme are in very close agreement. Thirty percent of grid points require a computationally expensive WENO-Z scheme for high-resolution capturing of shocks, whereas the remainder of grid points may be solved with the computationally more affordable central scheme. The computational cost of the Hybrid scheme can be up to a factor of one and a half lower as compared to computations with a WENO-Z scheme only for the sonic injector benchmark.

AMS subject classifications: 65P30, 77Axx

Key words: Weighted essentially non-oscillatory, central difference, multi-resolution, hybrid, shock, injector.

*Corresponding author.

Email: wsdon@hkbu.edu.hk (W. S. Don), gjacobs@mail.sdsu.edu (G. B. Jacobs)

1 Introduction

Conservative Weighted Essentially Non-Oscillatory finite difference schemes (WENO) have been developed in recent years as a class of high order (resolution) method for solutions of hyperbolic conservation laws (PDEs) in the presence of shocks and small scale structures in the solution (for a detail review of WENO schemes, see [1] and references contained therein). WENO schemes owe their success to the use of a dynamic set of substencils where a nonlinear convex combination of lower order polynomials *adapts* either to a higher order polynomial approximation at smooth parts of the solution, or to a lower order polynomial approximation that avoids interpolation across discontinuities. The upwinding of the spatial discretization provides the necessary dissipation for shock capturing.

The local computational stencils of $(2r - 1)$ order WENO schemes are composed of r overlapping substencils of r points, forming a larger stencil with $(2r - 1)$ points. The scheme yields a local rate of convergence that goes from order r at the non-smooth parts of the solution, to order $(2r - 1)$ when the convex combination of local lower order polynomials is applied at smooth parts of the solution. The nonlinear coefficients of WENO's convex combination, hereafter referred to as *nonlinear weights* ω_k , are based on lower order local smoothness indicators $\beta_k, k = 0, \dots, r - 1$ that measure the sum of the normalized squares of the scaled L^2 norms of all derivatives of r local interpolating polynomials. An essentially zero weight is assigned to those lower order polynomials whose underlining substencils contain high gradients and/or shocks, aiming at an essentially non-oscillatory solution close to discontinuities. At smooth parts of the solution, the formal order of accuracy is achieved through the mimicking of the central upwind scheme of maximum order, when all smoothness indicators are about the same size. Several techniques have been devised to design the nonlinear weights such as the original weights given in WENO-*JS* [1], the mapped weights given in WENO-*M* [3] and the optimal order weights given in WENO-*Z* [7, 8]. It has been shown that the new set of nonlinear weights of WENO-*Z* provided less dissipation than WENO-*JS* and yielded comparable resolution of smooth solution and captured sharp gradients as WENO-*M* [9–11]. In this study, we will employ the WENO-*Z* for our numerical experiments.

Following [7, 8], the hyperbolicity of the Euler equations admits a complete set of right and left eigenvectors for the Jacobian of the system. The approximated eigenvalues and eigenvectors are obtained via the Roe averaged Jacobian. The first order global Lax-Friedrichs flux is used as the low order building block for the high order reconstruction step of the WENO scheme. After projecting the positive and negative fluxes on the characteristic fields via the left eigenvectors, the high order WENO reconstruction step is applied (first/second) to obtain the high order approximation at the cell boundaries using the surrounding cell-centered values, which are then projected back into the physical space via the right eigenvectors and added together to form a high order numerical flux at the cell-interfaces. The conservative difference of the reconstructed high order fluxes then determines the divergence of the inviscid

Euler fluxes.

The procedure of the WENO scheme for finding the divergence of the Euler fluxes is computationally costly. Furthermore, in the physical regions where the solution is sufficiently smooth, the WENO procedure is unnecessary and should be avoided if and whenever possible. In smooth regions, a simple high order central finite difference scheme (C-FD) is computationally less expensive. Moreover, C-FD scheme has a lower numerical dissipation as compared to the WENO scheme. The challenge in adapting the solution solver from a high order WENO-Z in non-smooth regions to a high order C-FD scheme in smooth regions and vice versa, is that it needs to be done dynamically at each grid point and each time step and in a robust, consistent and computationally efficient manner. In order to maintain a good performance and high order accuracy of the divergence operator in the smooth regions, the algorithm must also be high order. In this study, we adopt the high order multi-resolution analysis algorithm (MR) by Harten [2]. While similar hybridization techniques have been developed with other finite difference/finite volume schemes, most of them were coupled with a low (first/second) order smoothness measurement algorithms (see [4–6, 15–17, 20, 21] and references contained therein for details) making them theoretically less efficient and less accurate than hybridizations that employ the *higher order* smoothness indicator.

A high order Hybrid scheme that switches between high order WENO-Z scheme and high order C-FD scheme based on the high order multi-resolution analysis was developed in *two-dimensions* in Costa and Don [4]. In this paper, we extend this Hybrid scheme to *three-dimensions* and we assess the performance of the Hybrid scheme in terms of speed and accuracy in parallel computations of a three dimensional circular sonic jet in supersonic cross flow following the benchmark experiment performed by Schetz [22]. The flow field is rich with many important features that are typical for sonic injection in supersonic cross stream (see Fig. 2) including shocks that form ahead of the injector; a large scale expansion plume ending originating from the injector and ending in a barrel shock and a reflected shock; and a highly unstable contact slip line (shear layer) that emanates from the edges of the injector leading to the formation of high-frequency small vortical structures. Hence, the flow contains all the flow structures and scales that the Hybrid scheme is particularly, ideally suited to compute in an accurate and efficient manner. We investigate the performance of the Hybrid scheme in terms of accuracy for long time integration and in terms of the efficiency measured with CPU timing running on a parallel machine. The Hybrid scheme is shown to be up to 40% more computationally efficient than the pure WENO scheme for the injector benchmark. The results computed with various orders of the Hybrid scheme and different grid resolutions are in good agreement with those computed with a pure WENO scheme. Since the dissipation and dispersion are slightly different, small differences in the generation and evolution of the small scale structures are observed along the unstable slip line between Hybrid scheme and pure WENO scheme computations.

In Section 2, a brief introduction to the Hybrid scheme and its algorithm is given. The central finite difference scheme, WENO finite difference scheme and the Multi-Resolution analysis are briefly described in Sections 2.1, 2.2 and 2.3 respectively. Sec-

tion 3 discusses the application of the Hybrid scheme to the three dimensional circular sonic jet injection into a supersonic cross flow. The computational results using both the pure WENO scheme and Hybrid scheme are presented and the performance of the Hybrid scheme is discussed. Conclusion and remarks are given in Section 4.

2 Hybrid Central-WENO finite difference scheme (Hybrid)

A hybrid scheme that hybridizes the high order non-dissipative central finite difference scheme (C-FD) and an improved high order weighted essentially non-oscillatory scheme (WENO-Z) presented in [4] is presented for solution of the three-dimensional Euler equations.

The well-known equations comprise a system of non-linear hyperbolic conservation laws that can be written compactly as

$$\frac{\partial \mathbf{Q}}{\partial t} + \nabla \cdot \mathbf{F}(\mathbf{Q}) = 0. \quad (2.1)$$

The system is discretized on a Cartesian uniformly spaced mesh in a three dimensional rectangular physical domain. The central finite difference scheme is employed in regions where the flow solution is smooth. The WENO-Z finite difference scheme is employed otherwise to capture discontinuities in the flow solution such as shocks and contact discontinuities whose formation is closely related to the nonlinear nature of (2.1). To determine the smoothness of solution in the computational domain and to maintain the high order (resolution) nature of the Hybrid scheme, the high order multi-resolution analysis (MR) by Harten [2] is employed to switch between C-FD and WENO schemes. The temporal and spatial adaptation of the two high order (resolution) schemes allows one to take advantages of the fast non-dissipative C-FD solver for an accurate and efficient long time simulations while sharp gradients and shocks are captured in an essentially non-oscillatory manner by the WENO scheme.

We briefly review the three individual high order (resolution) components of the Hybrid method, including the C-FD, WENO-Z, and MR schemes followed by a summary of the Hybrid algorithm. For a more detailed description, we refer to [4]. We present the schemes in one space dimension. Following a method of lines, the one-dimensional method extends naturally to multi-dimensions in Cartesian coordinates.

2.1 Central finite difference scheme (C-FD)

A central finite difference scheme (C-FD) of order n approximates the derivative of a function at a grid point x_i on a Cartesian uniformly spaced mesh as follows

$$\frac{d}{dx}f(x_i) = \frac{1}{\Delta x} \sum_{j=-n}^n w_j f_{i+j}, \quad (2.2)$$

where w_j are the Lagrangian weights of the first derivative [13].

Whereas the C-FD scheme is non-dissipative, it does suffer from numerical dispersive errors that introduce artificial high-frequency waves in the solution. To prevent these high-frequency oscillations from causing numerical instabilities, a high order smoothing is required to remove them. For a given function $f(x)$, discretized on a uniformly spaced grid, a filtered function of order n , $\hat{f}(x)$, at the grid point x_i can be expressed as

$$\hat{f}_i = \sum_{j=-n}^n \alpha_j f_{i+j}, \tag{2.3}$$

where α_j are the filtering weights which satisfy the symmetry property $\alpha_{-j} = \alpha_j$. The coefficients α_j are chosen in such a way that the first n moments of the filtered function match exactly the first n monomials $\{1, x, \dots, x^n\}$ ensuring that the approximation order of the filtered function is kept high. In addition to that, the α_j are also required to satisfy the condition

$$\sum_{j=-n}^n \alpha_j (-1)^j = 0,$$

so that oscillations at high wavenumbers are attenuated to zero. Some of these high order filtering weights α_j can be found in [14].

2.2 Weighted essentially non-oscillatory scheme (WENO)

WENO captures discontinuities in the flow solution in an essentially non-oscillatory manner and resolves the high frequency waves accurately. We consider the characteristics based weighted essentially non-oscillatory conservative finite difference scheme (WENO-Z) for the solution of the system of hyperbolic conservation laws of order, $(2r - 1)$. We present the explicit formula for a fifth ($r = 3$) order scheme. Extension to higher order ($r > 3$) WENO scheme is straightforward as explained in [8].

Consider a uniform spaced grid defined by the points $x_i = i\Delta x, i = 0, \dots, N$, which are called cell centers, with cell boundaries given by $x_{i+1/2} = x_i + \Delta x/2$, where Δx is the uniform grid spacing (see Fig. 1). The semi-discretized form of (2.1) is transformed into the system of ordinary differential equations and solved by the method

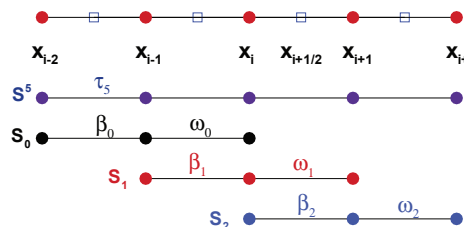


Figure 1: The computational uniformly spaced grid x_i and the 5-points stencil S^5 , composed of three 3-points substencils S_0, S_1, S_2 , used for the fifth-order WENO reconstruction step.

of lines

$$\frac{dQ_i(t)}{dt} = -\frac{\partial f}{\partial x}\Big|_{x=x_i}, \quad i = 0, \dots, N, \tag{2.4}$$

where $Q_i(t)$ is a numerical approximation to the cell-averaged value $Q(x_i, t)$. To form the flux differences across the uniformly spaced cells and to obtain high-order numerical fluxes consistent with the hyperbolic conservation laws, a conservative finite-difference formulation is required at the cell boundaries. We implicitly define the numerical flux function $h(x)$ as

$$f(x) = \frac{1}{\Delta x} \int_{x-\frac{\Delta x}{2}}^{x+\frac{\Delta x}{2}} h(\xi) d\xi, \tag{2.5}$$

such that the spatial derivative in (2.4) is approximated by a conservative finite difference formula at the cell boundaries x_i ,

$$\frac{du_i(t)}{dt} = -\frac{1}{\Delta x} (h_{i+\frac{1}{2}} - h_{i-\frac{1}{2}}), \tag{2.6}$$

where $h_{i\pm 1/2} = h(x_{i\pm 1/2})$. High order polynomial interpolations to $h_{i\pm 1/2}$ are computed using known cell-averaged values $f_j = f(x_j), j = i - r + 1, \dots, i + r - 1$.

The $(2r - 1)$ order WENO scheme uses a $(2r - 1)$ -points global stencil, which is subdivided into r substencils $\{S_0, S_1, \dots, S_{r-1}\}$ with each substencil containing r grid points and a global stencils $S^{2r-1} = \bigcup_{i=0}^{r-1} S_i$. For $r = 3$, the 5-points global stencil, hereafter named S^5 , is subdivided into three 3-points substencils $\{S_0, S_1, S_2\}$.

The $(2r - 1)$ degree polynomial approximation

$$\hat{f}_{i\pm\frac{1}{2}} = h_{i\pm\frac{1}{2}} + \mathcal{O}(\Delta x^{2r-1})$$

is built through the convex combination of the lower r degree polynomial $\hat{f}^k(x)$ in substencils S_k at the cell boundary $x_{i\pm 1/2}$:

$$\hat{f}_{i\pm\frac{1}{2}} = \sum_{k=0}^{r-1} \omega_k \hat{f}^k(x_{i\pm\frac{1}{2}}), \tag{2.7}$$

where

$$\hat{f}^k(x_{i+\frac{1}{2}}) = \sum_{j=0}^{r-1} c_{kj} f_{i-k+j}, \quad i = 0, \dots, N. \tag{2.8}$$

The c_{kj} are Lagrangian interpolation coefficients [1] and ω_k are normalized nonlinear weights (weights), which will be described below.

The regularity of the $(r - 1)$ degree interpolation polynomial approximation $\hat{f}^k(x)$ at the substencil S_k is measured by the lower order local smoothness indicators β_k , which are given by

$$\beta_k = \sum_{l=1}^{r-1} \Delta x^{2l-1} \int_{x_{i-\frac{1}{2}}}^{x_{i+\frac{1}{2}}} \left(\frac{d^l}{dx^l} \hat{f}^k(x) \right)^2 dx, \quad k = 0, \dots, r - 1. \tag{2.9}$$

For $r = 3$, the β_k in terms of the cell averaged values $f_i = f(x_i)$ are given explicitly by

$$\beta_0 = \frac{13}{12}(f_{i-2} - 2f_{i-1} + f_i)^2 + \frac{1}{4}(f_{i-2} - 4f_{i-1} + 3f_i)^2, \tag{2.10a}$$

$$\beta_1 = \frac{13}{12}(f_{i-1} - 2f_i + f_{i+1})^2 + \frac{1}{4}(f_{i-1} - f_{i+1})^2, \tag{2.10b}$$

$$\beta_2 = \frac{13}{12}(f_i - 2f_{i+1} + f_{i+2})^2 + \frac{1}{4}(3f_i - 4f_{i+1} + f_{i+2})^2. \tag{2.10c}$$

The WENO-Z scheme makes use of the higher order information obtained from a global optimal order smoothness indicator τ_{2r-1} which is built as a linear combination of β_k , that is,

$$\tau_{2r-1} = \left| \sum_{k=0}^{r-1} c_k \beta_k \right|, \tag{2.11}$$

where c_k are given constants [7,8]. For $r = 3$, one has $\tau_5 = |\beta_0 - \beta_2|$, which is of order $\mathcal{O}(\Delta x^5)$.

The normalized and un-normalized nonlinear weights ω_k^z and α_k^z , respectively, are defined as

$$\omega_k^z = \frac{\alpha_k^z}{\sum_{l=0}^{r-1} \alpha_l^z}, \quad \alpha_k^z = d_k \left(1 + \left(\frac{\tau_{2r-1}}{\beta_k + \epsilon} \right)^p \right), \quad k = 0, \dots, r-1. \tag{2.12}$$

The parameter ϵ (typically 10^{-12}) is used to avoid the division by zero in the denominator and power parameter p (typically $p = 2$) is chosen to increase the difference of scales of distinct weights at non-smooth parts of the solution. The coefficients $\{d_0, d_1, \dots, d_{r-1}\}$ are called the ideal weights since they generate the $(2r - 1)$ order central upwind scheme when the solution is smooth. For $r = 3$, the ideal weights are $\{d_0 = 3/10, d_1 = 3/5, d_2 = 1/10\}$.

Following [7, 8], the hyperbolicity of the Euler equations admits a complete set of right and left eigenvectors for the Jacobian of the system. The approximated eigenvalues and eigenvectors are obtained via the Roe averaged Jacobian. The first order global Lax-Friedrichs flux is used as the low order building block for the high order reconstruction step of the WENO scheme. After projecting the positive and negative fluxes on the characteristic fields via the left eigenvectors, the high order WENO reconstruction step is applied to obtain the high order approximation at the cell boundaries using the surrounding cell-centered values, which are then projected back into the physical space via the right eigenvectors and added together to form a high order numerical flux at the cell-interfaces. The conservative difference of the reconstructed high order fluxes can then be computed for inviscid flux.

The resulting system of ordinary differentiation equations ODE (2.2) and (2.6) remain after the spatial discretization are advanced in time via the third order TVD Runge-Kutta scheme [7]. The CFL condition is set to be $\text{CFL} = 0.45$ in the numerical experiments performed in this study.

2.3 Multi-Resolution analysis (MR)

The Multi-Resolution analysis (MR) measures the smoothness of the solution at each grid point at a given time and quantifies the smoothness through a MR coefficient. Since the WENO-Z and C-FD schemes are both high order schemes, the measure of the smoothness of the solution must also be of high order in order to differentiate a high frequency wave from a high gradient/shock so that the appropriate numerical spatial scheme (C-FD for high-frequency wave or WENO-Z for shocks) can be applied at a given spatial location and at a given time. To do so, the high order multi-level Multi-Resolution (MR) algorithm by Harten [2] is employed to detect the smooth and rough parts of the solution.

Given an initial number of the grid points N_0 and grid spacing Δx_0 , we shall consider a set of nested dyadic grids up to level $L < \log_2 N_0$,

$$G^k = \{x_j^k, j = 0, \dots, N_k\}, \quad 0 \leq k \leq L, \quad (2.13)$$

where $x_j^k = j\Delta x_k$ with $\Delta x_k = 2^k \Delta x_0$, $N_k = 2^{-k} N_0$ and the cell averages of function u at x_j^k :

$$\bar{u}_j^k = \frac{1}{\Delta x_k} \int_{x_{j-1}^k}^{x_j^k} u(x) dx. \quad (2.14)$$

Let \tilde{u}_{2j-1}^k be the approximation to \bar{u}_{2j-1}^k by a unique polynomial of degree $2s$ that interpolates \bar{u}_{j+l}^k , $|l| \leq s$ at x_{j+l}^k , where $r = 2s + 1$ is the order of approximation.

The approximation error (or multi-resolution coefficients) $d_j^k = \bar{u}_{2j-1}^{k-1} - \tilde{u}_{2j-1}^{k-1}$, at the k level and the grid point x_j , has the property that if $u(x)$ has $(p - 1)$ continuous derivatives and a jump discontinuity at its p derivative ($[\cdot]$ and (\cdot) denote the jump and the derivatives of the function respectively), then

$$d_j^k \approx \begin{cases} [u^{(p)}] \Delta x_k^p, & p \leq r, \\ u^{(r)} \Delta x_k^r, & p > r. \end{cases} \quad (2.15)$$

The multi-resolution coefficient d_j^k measures how close the data at the finer grid $\{x_j^{k-1}\}$ can be interpolated by the data at the coarser grid $\{x_j^k\}$. From (2.15) it follows that

$$|d_{2j}^{k-1}| \approx 2^{-\bar{p}} |d_j^k|, \quad \bar{p} = \min\{p, r\}, \quad (2.16)$$

which implies that away from discontinuities, the MR coefficients $\{d_j^k\}$ diminish in size with the refinement of the grid at smooth parts of the solution; close to discontinuities, they remain the same size, independent of the order $r = 2s + 1$ and level k of multi-resolution analysis. Since in this work, the first level ($k = 1$) MR coefficients $\{d_j^1\}$ are more than sufficient in detecting high gradients and shocks, we will drop the superscript 1 from the d_j^1 unless noted otherwise. Examples of the performance of

the high order multi-level multi-resolution analysis in detecting discontinuities in the solution of nonlinear system of hyperbolic PDE can be found in [4].

The computational overhead of the multi-resolution analysis, which comprises a dot product of a two vectors of length equal to the order of the MR analysis at each grid point in each dimension of a single flow quantity only once before the Runge-Kutta time stepping scheme, is negligible. It is equivalent to doing three more derivatives using C-FD scheme in each Runge-Kutta step and its cost is insignificant when compared to the cost of finding a non-oscillatory representation of the derivative of the flux by the WENO scheme. The enhanced solution is well worth the minor additional CPU time.

2.4 Hybrid scheme

Algorithmically, the Hybrid scheme is implemented with the following essential steps:

Step 1 The multi-resolution analysis (MR) is performed in a given variable (usually density) only once at the beginning of the Runge-Kutta TVD time stepping scheme.

A grid point is flagged as non-smooth based on the smoothness sensor

$$\text{Flag}_i = \begin{cases} 1, & |d_i| > \epsilon_{MR}, \\ 0, & \text{otherwise,} \end{cases} \quad (2.17)$$

where ϵ_{MR} is a user tunable parameter.

Step 2 A buffer zone is created around each grid point that is flagged as non-smooth.

If, for example, grid point, x_i , is flagged as non-smooth, then its

$$m = \beta \frac{1}{2} \max(N_c, N_w + 1),$$

where $\beta \geq 0$, N_c and N_w are the buffer zone factor, the order of C-FD scheme and the order of WENO scheme, respectively, neighboring points $\{x_{i-m}, \dots, x_i, \dots, x_{i+m}\}$ will also be designated as non-smooth, that is, $\{\text{Flag}_j = 1, j = i - m, \dots, i, \dots, i + m\}$. This condition prevents computation of the divergence of the Euler fluxes by the C-FD scheme using non-smooth functional values.

Step 3 The C-FD scheme, which is computationally more efficient than WENO scheme, will compute the divergence of the flux over the full computational domain first. Then, the WENO scheme is employed to overwrite the divergence of the flux at those grid points designated as non-smooth by the flag.

Remark 2.1. Since the WENO coverage of the solution is USUALLY smaller than the C-FD coverage, and since the C-FD can be vectorized in a cache efficient manner along lines, it is logical to compute the redundant C-FD solution that is going to be discarded and overwritten by the WENO scheme later. Moreover, ease of programming and implementation should be considered. From experience, we know that the additional program complexity and additional labor cost is too high and the gain is too small to justify a more elaborate implementation. Of course, there are exceptions and those cases should be evaluated on a case by case basis. At the end of the day, it is the WALL clock time that should be improved.

Remark 2.2. It is generally known that WENO scheme is approximately five times more expensive than the corresponding C-FD scheme with similar order. According to the paper by Johnsen et al. [12], they estimated the number of operations per grid point for C-FD6, C-FD8, WENO5 and WENO7 are 1100, 1600, 3100 and 6200 respectively, in computing the divergence of the convective fluxes. Since a WENO scheme is required to perform substantially more computations such as those involved in forming of the eigensystem, flux splitting and forward and backward characteristic projections, five times more CPU time is a reasonable estimate. Of course, the actual efficiency of any implementation of the scheme is also highly depended on the competency of the programmer and data structures.

Remark 2.3. The class of problems studied is restricted to those where the boundary conditions do not present any complications with the ghostpoints, for instance, periodic or freestream boundary conditions. In this work, we shall use as many ghostpoints as required for a given order of the C-FD scheme, the WENO scheme and the MR analysis. Also, the parameters $\epsilon_{MR} = 1 \times 10^{-4}$ and $\beta = 1$ are used typically.

3 Numerical results

The Hybrid scheme is tested on a three dimensional circular sonic jet injection in a Mach 2.1 supersonic cross flow with air according to the benchmark experiment performed by Schetz [22] and the computations performed later by Viti [23]. In the experiment a circular nozzle connects to a flat plate that is mounted parallel to the incoming supersonic flow. The flow field, as summarized in the schematic in Fig. 2, shows many flow features that are typical for sonic injection in supersonic cross stream. They include a laminar boundary layer that forms along the flat plate and a bow shock that forms ahead of the injector. The injected air at sonic speed expands rapidly into a plume and forms a barrel shock and a reflected shock. A contact slip line (shear layer) that emanates from the injector edge is highly unstable and leads to the formation of small, unsteady vortex structures. The interaction between the bow shock and the boundary layer further leads to form a local separation of the laminar boundary layer underneath the bow shock.

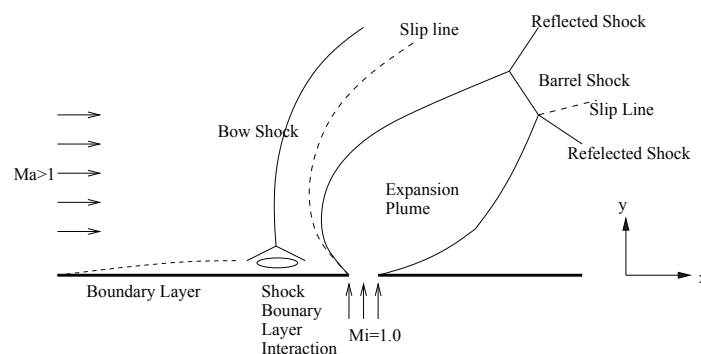


Figure 2: Schematic of flow features in a sonic injection in supersonic cross stream air flow.

Since the viscous effects are relatively small and since we are primarily interested in the performance of the Hybrid scheme in terms of accuracy and computational speed in this work, we compute the Schetz injector with the Hybrid *inviscid* Euler code. Since viscous effects are not accounted for, we are not able to capture the laminar boundary layer on the plate and the shock-boundary layer interaction. These viscous flow phenomena have only a minor influence on the large shock-expansion structures (bow shock, barrel shock, reflected shock, expansion plume and slip lines or shear layers). Moreover, with a high order Euler solver we are able to capture the more important small scale mixing structures in the unstable shear layers.

We consider a three dimensional rectangular domain with a supersonic cross-stream flow in x -direction and the sonic injection in y -direction. The rectangular computational domain size in x -, y - and z -direction is $(4\text{cm} \times 1.5 \times 1\text{cm})$ with the origin located at $(x_0, y_0, z_0) = (-2\text{cm}, 0\text{cm}, -0.5\text{cm})$. The freestream Mach number, pressure and temperature are $\text{Ma}_\infty = 2.1$, $p_\infty = 11.1\text{KPa}$ and $T_\infty = 159\text{K}$, respectively. The injection Mach number, pressure and temperature are $\text{Ma}_i = 1$, $p_i = 364.8\text{KPa}$, and $T_i = 250\text{K}$, respectively. The circular injector nozzle has a diameter of $d_n = 0.389\text{cm}$ with the center located at $(x_c, y_c, z_c) = (0\text{cm}, 0\text{cm}, 0\text{cm})$. Computations were performed with non-dimensionalized variables based on a reference time scale of $t_{ref} = 3.95 \times 10^{-5}\text{s}$. The final non-dimensional time of $T_f = 3$ time units or in dimensional units, $T_f = 1.2 \times 10^{-4}\text{s}$, is sufficiently long for the flow to reach a quasi-steady state in which most large scale structures are statistically invariant.

Free-stream conditions are specified at the x faces of the computational domain according to the supersonic cross-stream flow. In the z -direction, periodic boundary conditions are specified. On the bottom and top y -planes, a symmetry or zero mass flux condition is specified. The injector boundary condition is specified on ghost points (similar to the free stream conditions) and on grid points that are located within the circular injector region. The circular injector boundary geometry is hence an approximated through a staircasing approximation in the Cartesian grid.

Three grid sizes as described in Table 1 were considered. The variables N_x , N_y and N_z denote the number of uniformly spaced grid points in the x -, y - and z -directions, respectively. Computations are performed with the Hybrid scheme, with approximation orders of $2r - 1 = 3, 5$ and 7 for WENO 4, 6 and 8 for C-FD. We shall denote Hybrid-CnWmMkGi as an n order C-FD scheme, a m order WENO-Z scheme and a k order MR analysis at a grid resolution case i in the following discussion. For example, Hybrid-C8W7M8G3 means the Hybrid scheme with an eighth order C-FD scheme, a seventh order WENO-Z scheme and an eighth order MR analysis at a grid resolution

Table 1: Grid sizes used in the computation of the jet interaction in a Mach 2.1 supersonic cross flow with air.

Grids	N_x	N_y	N_z
1	360	135	90
2	400	150	100
3	444	167	111

$(N_x, N_y, N_z) = (444, 167, 111)$. In general, for a given $M = 2r - 1$ order WENO-Z scheme, we will set $n = k = m + 1$ in the computations performed in this study. An $n + 2$ order smoothing of the solution in the smooth regions of the domain is performed at the end of a Runge-Kutta TVD time stepping.

To avoid large and complicated three dimensional plots, that do not add significantly to the performance assessment of the Hybrid scheme, we focus on the visualization of flooded contour fields of relevant variables (mainly, density ρ , Mach number Ma and vorticity ω) with a two dimensional $x - y$ plane cut at the center $z = z^* = 0\text{cm}$ of the three dimensional physical domain.

The three dimensional simulations of this problem capture the evolution of the small scale eddies along the unstable slip line that plays an important role in the formation of transverse vortex tubes around the injecting jet. In Fig. 3, the temporal evolution of the density $\rho(x, y, z^*, t_n)$ and Mach number $Ma(x, y, z^*, t_n)$ are shown via a two dimensional $x - y$ plane cut with $z = z^* = 0\text{cm}$ as well as the three dimensional two levels iso-surfaces of the Mach number Ma , from early times t until the final time $t = 3$, as computed by the Hybrid-C8W7M8G3 scheme. The Hybrid scheme captures the long time evolution of the large scales structures (bow shock, barrel shock, reflected shock and expansion plume) as well as the small scales eddies structures (vortical rollups along the slip line) in an accurate and efficient manner as we will discuss in detail below. The instabilities near the base of the injector jet lead to the formation of coherent structures between the bow shock and the expansion plume.

To justify the use of the high order (resolution) Hybrid scheme, we plot, in Fig. 4, the two dimensional density contour fields with increasing grid resolutions in the x -direction by 100 grid points and with increasing order of the WENO-Z scheme from the $m = 2r - 1 = 3, 5$ and 7 with corresponding order of the C-FD scheme and the MR analysis as discussed above. The low order and low grid resolution Hybrid scheme fails to capture the small scales eddies along the unstable slip lines but perform much better with increasing order and grid resolution. For low order scheme, the high numerical dissipation inherited in the underlying scheme requires a significant grid refinement to capture the small scales eddies. However, the increasing of grid resolution imposes a severe stress on the computational hardware in terms of memory and CPU time. It is recommended that high order scheme should be used whenever possible for accurate capturing of small scales structures in a long time flow evolution.

In Fig. 5, the density ρ , Mach number Ma and vorticity ω contours are visualized at $t=3$ as computed via a pure WENO-Z scheme and the Hybrid scheme with various orders with a fixed grid resolution $(N_x, N_y, N_z) = (444, 167, 111)$. The large scales structures in Hybrid and pure WENO computations are in good agreement except for minor differences in the small scales structures along the unstable slip lines between the bow shock and the expansion plume. The minor differences are a result of the slightly different level of dissipation in the WENO and C-FD schemes at the same grid location and time. This translates in a slightly different flow behavior of the small scales structures even if they are evolved in time by the same time stepping scheme. Similar results and remarks are obtained with other grid resolutions (not shown).

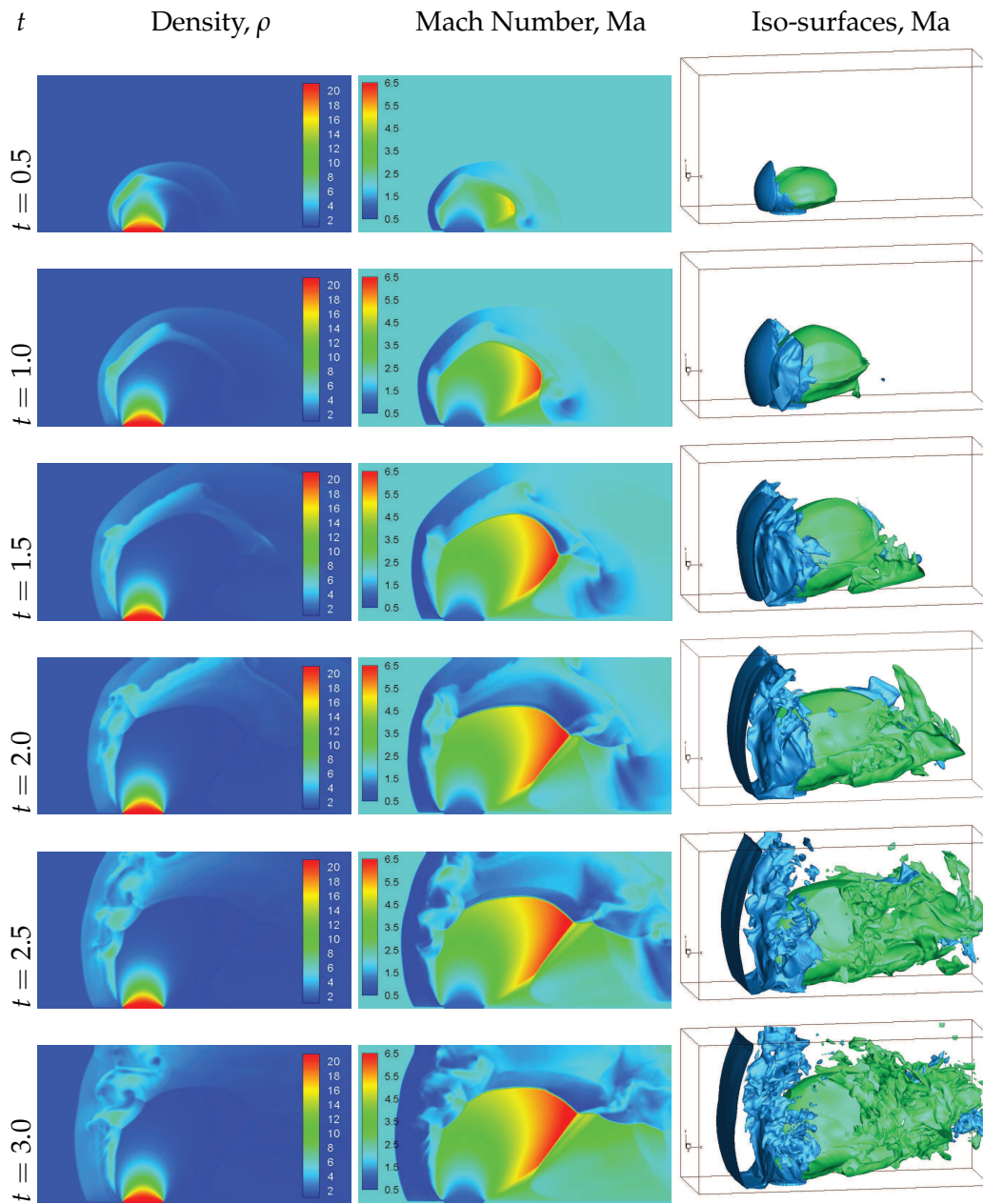


Figure 3: Temporal evolution of density ρ (left column) and Mach number Ma (middle column) at the center $z^* = 0\text{cm}$ are shown at various times as computed by the Hybrid-C8W7M8G3 scheme. The iso-surfaces of the Mach number (right column) are also given.

Computations were performed on an eight nodes cluster with 8 Intel Xeon cores per node at a clock speed of 2.5GHz. All computations were run on eight cores. The computational domain with uniform grid spacing was partitioned using Cartesian domain decomposition. The parallel speed-up for this code and case up to eight pro-

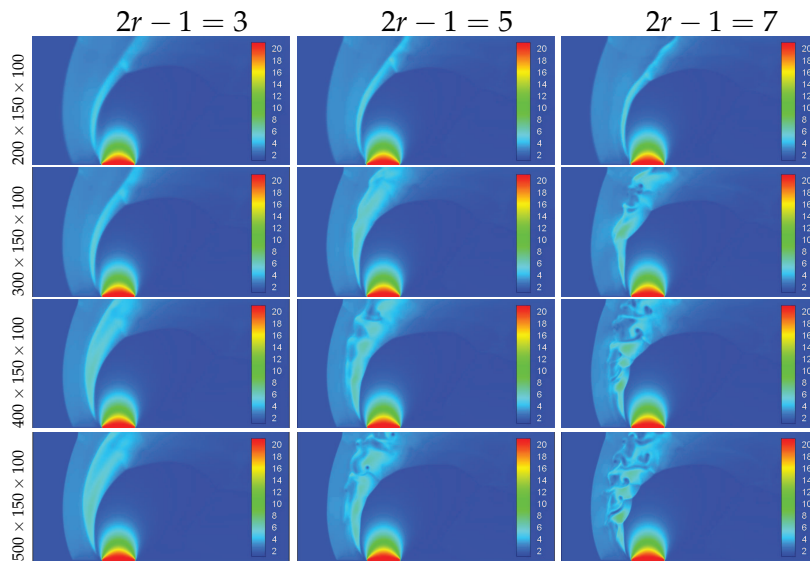


Figure 4: The two dimensional $x - y$ plane cut of the density fields as computed by the Hybrid scheme with various orders and grid resolutions at time $t = 3$.

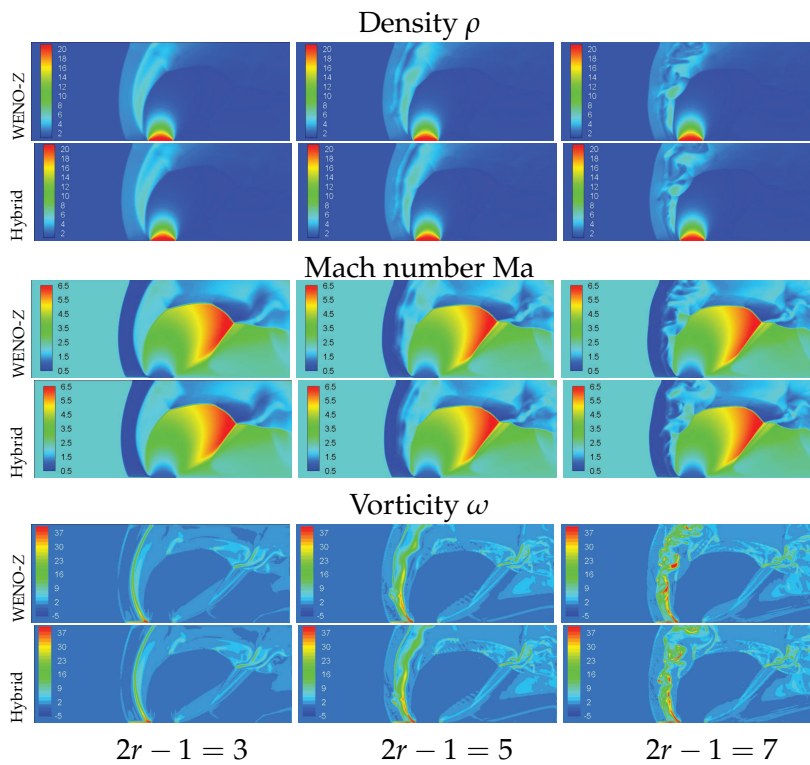


Figure 5: The two-dimensional $x - y$ plane cut of density ρ , Mach number Ma and vorticity ω as computed by a pure WENO-Z scheme and the Hybrid scheme with various orders at time $t = 3$. The grid resolution is $(N_x, N_y, N_z) = (444, 167, 111)$.

Table 2: Timing in hours of the simulations at $t = 1$ with a pure WENO-Z scheme and a Hybrid scheme of various orders and grid resolutions. The speed up in percentage is also given inside the parenthesis.

Cases	$2r - 1 = 3$		$2r - 1 = 5$		$2r - 1 = 7$	
	WENO	Hybrid	WENO	Hybrid	WENO	Hybrid
(a) $360 \times 135 \times 90$	2.8	2.2 (27%)	3.6	2.6 (38%)	4.5	3.1 (45%)
(b) $400 \times 150 \times 100$	4.2	3.3 (27%)	5.4	3.7 (46%)	6.8	4.5 (51%)
(c) $444 \times 167 \times 111$	6.5	4.9 (33%)	8.2	5.6 (46%)	10.3	6.6 (56%)

processors is ideal. The CPU timing of the runs to time $t = 1$ is shown in Table 2.

On average the Hybrid scheme is 40% faster than the pure WENO-Z scheme. The Hybrid scheme, on average, has a 35% coverage of WENO-Z scheme and hence a 65% coverage of the C-FD scheme. With an increase of grid size from the coarse grid (a) to the fine grid (c) in Table 2, the percentage of WENO-Z coverage reduces as shown in the bar-plot in Fig. 6. The reduced WENO-Z coverage lowers the normalized computational cost as shown versus the normalized grid size for different order $2r - 1 = 3, 5$ and 7 in Fig. 6. At large orders, $2r - 1$, the reduction in WENO-Z coverage leads to a relatively larger increase in efficiency of the Hybrid as compared to the pure WENO-Z. At $2r - 1 = 7$ and for the finest grid (c), the Hybrid improves the computational efficiency by 56%.

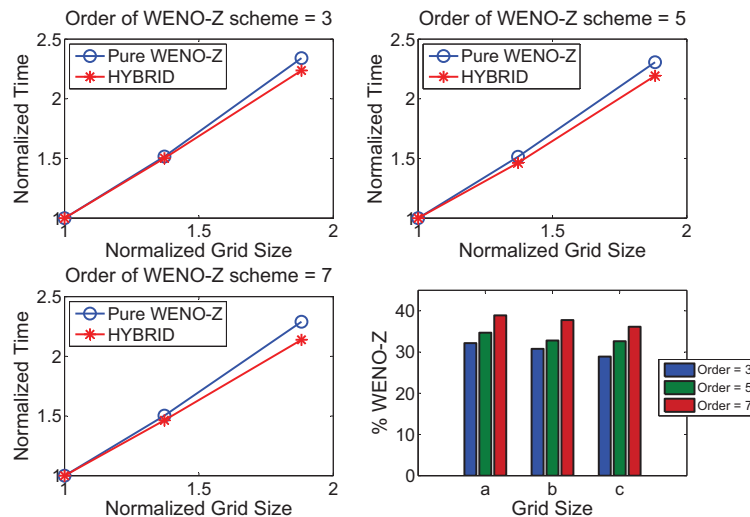


Figure 6: Comparison of timing results and percentage of WENO coverage used by the Hybrid scheme.

We note that with an increase in approximation order from $2r - 1 = 3$ to 7 , the WENO-Z coverage increases by approximately 10% (bar-plot in Fig. 6). This means that the Hybrid scheme is relatively less efficient with increasing order because of the increased WENO coverage.

Remark 3.1. The overall efficiency of Hybrid scheme is highly problem dependent, in some particular problems at a given time when the WENO coverage of the solution is

highly fragmented such as the problem studied here, one cannot expect high computational efficiency due to the lack of vectorization, frequent cache dump and memory reload. This is an active area of research to alleviate this aspect of Hybrid scheme by the authors.

4 Conclusions

The high order Hybrid WENO-Central finite difference Euler Solver is extended from two to three dimensions. The parallelized Hybrid scheme was tested on a sonic injector benchmark flow in supersonic cross stream.

The Hybrid scheme uses the WENO-Z scheme in regions of the physical domain where the flow is not smooth and contains discontinuities such as contact discontinuities and shocks, whereas in smooth regions it uses a central finite difference scheme. The smoothness of the solution is quantified with a multi-resolution coefficient that is determined through a high order multi-resolution analysis on a single solution variable. Based on the multi-resolution coefficient, the Hybrid scheme switches dynamically between the computationally efficient central finite difference scheme and the computational more expensive WENO-Z scheme at each grid point and at each time step. The computational overhead of the multi-resolution analysis, which comprises a dot product of a two vectors of length equal to the order of the MR analysis at each grid point in each dimension of a single flow quantity before each Runge-Kutta time stepping scheme, is negligible as compared to the cost of finding a non-oscillatory representation of the derivative of the flux by the WENO scheme. The Hybrid scheme is hence more computationally efficient.

To illustrate the accuracy and efficiency, the Hybrid scheme was tested by means of computations of the benchmark flow problem of the sonic injection of fluid into a supersonic cross stream flow. The computations focused on a near injector flow region which features rich interaction between both large-scale shocks and expansions and the growth of small scale flow instabilities. In the initially uniform supersonic flow, the curved cross stream jet increasingly blocks the flow and as a result instabilities and shocks develop ahead and along of the curved cross-stream jet. Since the pressure of the jet is higher than the pressure in the cross stream, the jet expands and accelerates creating additional instabilities downstream, until it reaches a quasi-steady state.

For this flow computation 30% of the computational domain requires the use of WENO-Z scheme. With this a relatively large percentage of WENO-Z usage, the computation is up to 1.56 times faster with the Hybrid scheme than the one with a pure WENO-Z scheme. With increasing grid resolution, the WENO-Z coverage becomes relatively smaller, and the Hybrid scheme becomes relatively more efficient. For large computational domains, the lesser WENO-Z coverage is needed and hence computational cost should decrease further. On average the speed up with Hybrid scheme is 40% for the cases considered in this paper.

The flows computed with a Hybrid scheme and with a pure WENO-Z scheme are

in very good agreement. Hence, while the Hybrid scheme improves computational efficiency over the high order WENO-Z scheme, it does not reduce the accuracy. If anything, it is expected that the Hybrid scheme is more accurate, since the numerical dissipation and dispersion of the central difference schemes are smaller than WENO-Z scheme.

With an increasing order of underlying schemes, the capturing of the growth of small scale instabilities improves. With a third order scheme, the shear layer emanating from the injector jet is stable whereas at the fifth and seventh order scheme, the shear layer is unstable. Effectively, a lesser grid resolution is required with an increased order of approximation to obtain the same result. The lesser grid resolution reduces computational cost, which reduces the computational time by a factor that is dependent on the problem as well as choice of parameters of the numerical scheme. For the injector cases, with an increase of the order of approximation by two orders, similar results are obtained for grid resolution that require only half the computational time, i.e., another factor 2 of relative increase in computational efficiency.

In near future work, we plan to develop the Hybrid scheme for the solution a full three-dimensional Navier-Stokes equations to include the viscous and heat conduction effects in this class of problems. The Hybrid scheme for Navier-Stokes equations will enable the study of viscous effects, such as shock-boundary layer interaction, on the sonic injection in supersonic cross stream.

Acknowledgments

We would like to acknowledge the funding support of this research by the RGC grant HKBU-200910 from Hong Kong University Grant Council (Don), an AFOSR-Young Investigator Grant (AFOSR-F9550-09-1-0097), the support by NSF (NSF-DMS-1115705) and the Computational Science Research Center at SDSU (Jacobs). We further extend our gratitude to Prof. Parra at the University of Valladolid for her efforts in the exchange program of students between the University of Valladolid and San Diego State University.

References

- [1] C. W. SHU, *High order weighted essentially non-oscillatory schemes for convection dominated problems*, SIAM Rev., 51 (2009), pp. 82–126.
- [2] A. HARTEN, *High resolution schemes for hyperbolic conservation laws*, J. Comput. Phys., 49 (1983), pp. 357–393.
- [3] A. K. HENRICK, T. D. ASLAM AND J. M. POWERS, *Mapped weighted essentially non-oscillatory schemes: achieving optimal order near critical points*, J. Comput. Phys., 207 (2005), pp. 542–567.
- [4] B. COSTA AND W. S. DON, *High order Hybrid Central-WENO finite difference scheme for conservation laws*, J. Comput. Appl. Math., 204(2) (2007), pp. 209–218.

- [5] B. COSTA AND W. S. DON, *Multi-domain hybrid spectral-WENO methods for hyperbolic conservation laws*, J. Comput. Phys., 224(2) (2007), pp. 970–991.
- [6] B. COSTA, W. S. DON, D. GOTTLIEB AND R. SENDERSKY, *Two-dimensional multi-domain hybrid spectral-WENO methods for conservation laws*, Commun. Comput. Phys., 1(3) (2006), pp. 548–574.
- [7] R. BORGES, M. CARMONA, B. COSTA AND W. S. DON, *An improved weighted essentially non-oscillatory scheme for hyperbolic conservation laws*, J. Comput. Phys., 227 (2008), pp. 3101–3211.
- [8] M. CASTRO, B. COSTA AND W. S. DON, *High order weighted essentially non-oscillatory WENO-Z schemes for hyperbolic conservation laws*, J. Comput. Phys., 230 (2011), pp. 1766–1792.
- [9] Z. GAO, W. S. DON AND Z. LI, *High order weighted essentially non-oscillation schemes for one-dimensional detonation wave simulations*, J. Comput. Math., 29(6) (2011), pp. 623–638.
- [10] Z. GAO, W. S. DON AND Z. LI, *High order weighted essentially non-oscillation schemes for two-dimensional detonation wave simulations*, J. Sci. Comput., DOI: 10.1007/s10915-011-9569-0, 2012.
- [11] M. LATINI, O. SCHILLING AND W. S. DON, *Effects of order of WENO flux reconstruction and spatial resolution on reshocked two-dimensional Richtmyer-Meshkov instability*, J. Comput. Phys., 221 (2007), pp. 805–836.
- [12] E. JOHNSEN, J. LARSSON, A. V. BHAGATWALA, W. H. CABOT, P. MOIN, B. J. OLSON, P. S. RAWAT, S. K. SHANKAR, B. SJOGREEN, H. C. YEE, X. ZHONG AND S. K. LELE, *Assessment of high-resolution methods for numerical simulations of compressible turbulence with shock waves*, J. Comput. Phys., 229 (2010), pp. 1213–1237.
- [13] B. FORNBERG, *Calculation of weights in finite difference formulas*, SIAM Rev., 40(3) (1998), pp. 685–691.
- [14] O. VASILYEV, T. LUND AND P. MOIN, *A general class of commutative filters for LES in complex geometries*, J. Comput. Phys., 146(1) (1998), pp. 82–104.
- [15] N. ADAMS AND K. SHARIFF, *High-resolution hybrid compact-ENO scheme for shock-turbulence interaction problems*, J. Comput. Phys., 127 (1996), pp. 27–51.
- [16] D. HILL AND D. PULLIN, *Hybrid tuned center-difference-WENO method for large eddy simulations in the presence of strong shocks*, J. Comput. Phys., 194 (2004), pp. 435–450.
- [17] S. PIROZZOLI, *Conservative hybrid compact-WENO schemes for Shock-Turbulence interaction*, J. Comput. Phys., 178(1) (2002), pp. 81–117.
- [18] D. W. ZINGG, *Comparison of high-accuracy finite difference methods for linear wave propagation*, SIAM J. Sci. Comput., 22(2) (2000), pp. 476–502.
- [19] C. BOGEY AND C. BAILLY, *A family of low dispersive and low dissipative explicit schemes for flow and noise computations*, J. Comput. Phys., 194 (2004), pp. 194–214.
- [20] A. CHOEN, S. M. KABER, S. MULLER AND M. POSTEL, *Fully adaptive multiresolution finite volume schemes for conservation laws*, Math. Comput., 72(241) (2001), pp. 183–225.
- [21] B. BIHARI AND A. HARTEN, *Multiresolution schemes for the numerical solution of 2-D Conservation Laws*, SIAM J. Sci. Comput., 18(2) (1997), pp. 315–354.
- [22] J. A. SCHETZ, P. F. HAWKINS AND H. LEHMAN, *Structure of highly under-expanded transverse jets in a supersonic stream*, AIAA J., 35(5) (1976), pp. 882–884.
- [23] V. VITI, *Numerical Analysis of the Jet Interaction Flowfield with a Main Jet and an Array of Smaller Jets*, Ph.D. dissertation, Virginia Tech, 2002.